

Supporting Information

for

***1-D Coordination Polymer Route to Catalytically Active Co@C Nanoparticles***

Anand Pariyar,<sup>a</sup> Siddharth Gopalakrishnan,<sup>b</sup> Joseph Stansbery,<sup>b</sup> Rajankumar L. Patel,<sup>b</sup> Xinhua Liang,<sup>b</sup> Nikolay Gerasimchuk<sup>c</sup> and Amitava Choudhury<sup>a,\*</sup>

\*E-mail: [choudhurya@mst.edu](mailto:choudhurya@mst.edu)

<sup>a</sup>Department of Chemistry, Missouri University of Science and Technology, Rolla , 400-W 11<sup>th</sup> Street, Rolla, MO 65409, USA. Fax: +1-573-341-6033; Tel: +1-573-341-6332.

<sup>b</sup>Department of Chemical and Biochemical Engineering, Missouri University of Science and Technology, Rolla, MO 65409, USA.

<sup>c</sup>Department of Chemistry, Missouri State University, Springfield, MO 65897, USA.

**Table of Content:**

<b>Sl. No</b>	<b>Content</b>	<b>Page No</b>
<b>1</b>	Table S1: Selected bond lengths and angles from compound <b>1</b>	<b>S3</b>
<b>2</b>	Table S2. CH... $\pi$ interaction in 1-D Co-Polymeric complex <b>1</b>	<b>S3</b>
<b>3</b>	Table S3. H-bonding interaction in 1-D Co-Polymeric complex <b>1</b>	<b>S3</b>
<b>4</b>	Fig S1: FT-IR spectrum of <b>1</b> in KBr disc.	<b>S4</b>
<b>5</b>	Fig. S2: TGA profile of as synthesized <b>1</b> under N <sub>2</sub> flow	<b>S4</b>
<b>6</b>	Fig. S3: Physical separation of a suspension of <b>2</b> in ethanol a magnet.	<b>S5</b>
<b>7</b>	Fig. S4: Electron diffraction pattern of a single Co nanoparticle	<b>S5</b>
<b>8</b>	Fig. S5. TEM image of <b>2</b>	<b>S6</b>
<b>9</b>	Fig. S6. Cobalt 2p XPS spectrum of <b>2</b>	<b>S6</b>
<b>10</b>	Fig. S7: Reduction of PNP to PAP with <b>1</b> , <b>2</b> and blank	<b>S7</b>
<b>11</b>	Table S4: Comparison of rate constants for support and supported catalyst	<b>S7</b>
<b>12</b>	Fig. S8: Reduction of PNP to PAP with <b>2</b> (red line) and in absence of any catalyst (black square).	<b>S8</b>
<b>13</b>	Table S5: Comparison of activation energy among metal supported nanoparticles.	<b>S8</b>
<b>14</b>	Fig. S9: Pore width calculated for Co@C ( <b>2</b> )	<b>S9</b>
<b>15</b>	References	<b>S10</b>

Table S1: Selected bond lengths and angles from compound **1**

Co(1)-O(3)	2.007(2)	Co(1)-N(3)	2.029(2)
Co(1)-O(1)	2.0083(18)	Co(1)-N(1)	2.056(2)
O(3)-Co(1)-O(1)	99.98(9)	O(3)-Co(1)-O(1)	99.98(9)
O(3)-Co(1)-N(3)	128.46(10)	O(3)-Co(1)-N(3)	128.46(10)
O(1)-Co(1)-N(3)	117.77(8)	O(1)-Co(1)-N(3)	117.77(8)

Table S2. Non-covalent CH... π Interaction in 1-D Co-Polymeric complex **1**.

CH... π Interaction in <b>1</b>			
X-H...Cg(J)	d(H....Cg) Å	γ-angle (°)	Symmetry code
C(7)-H(7A)...Cg(3)	2.93	9.24	[1655.01]
C(3)-H(3A)...Cg(4)	2.84	5.01	[1655.01]
C(9)-H(9A)...Cg(5)	2.93	18.53	[1455.01]

Cg(J) = center of gravity of ring J; γ-angle = angle between Cg-H vector and ring J normal.  
 Centroid: Cg(3) = N(1)-C(9)-N(2)-C(10)-C(11), Cg(4) = N(3)-C(13)-N(4)-C(14)-C(15),  
 Cg(5) = C(2)-C(3)-C(4)b-C(2)b-C(3)b-C(4). [1455] = -1+x,y,x; [1655] = 1+x,y,z.

Table S3. Non-covalent H-bonding interaction in 1-D Co-Polymeric complex **1**.

H-bonding Interaction in <b>1</b>			
D-H...A	d(H...A) Å	D-H...A angle (°)	Symmetry code
C(10)-H(10A)..O(2)	2.56	167	[ 1465.01]
C(12)-H(12C)..O(1)	2.55	160	[2665.01]

D-H...A= Donor-Hydrogen...Acceptor; [1465]=1-x,1-y,-z; [2665]=- 1+x,1+y,z.

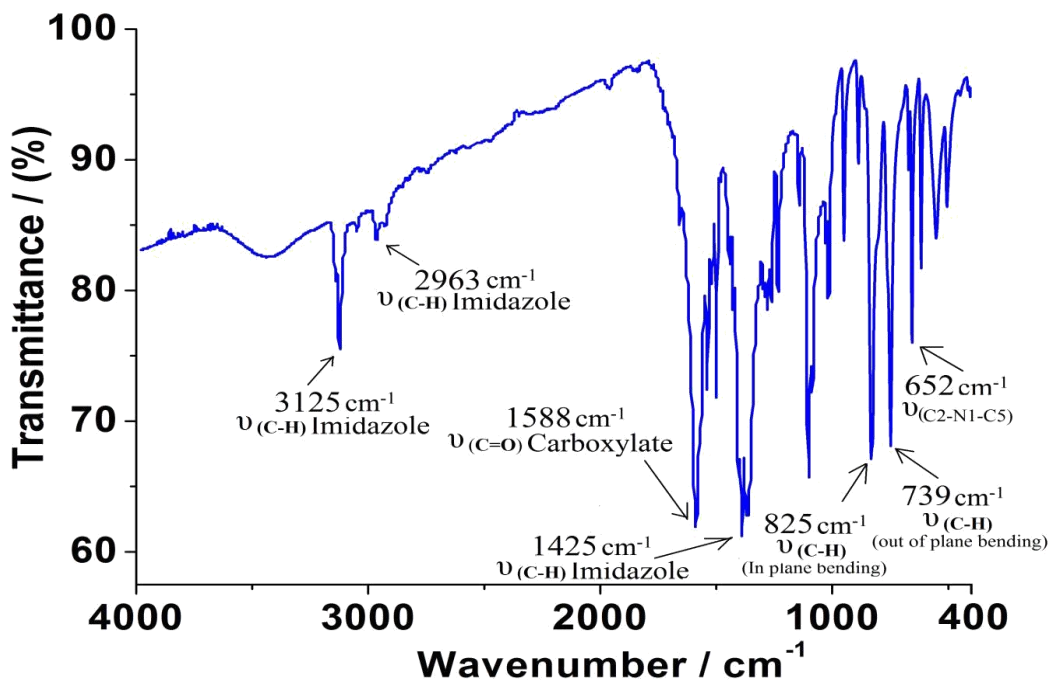


Fig S1: FT-IR spectrum of **1** in KBr disc.

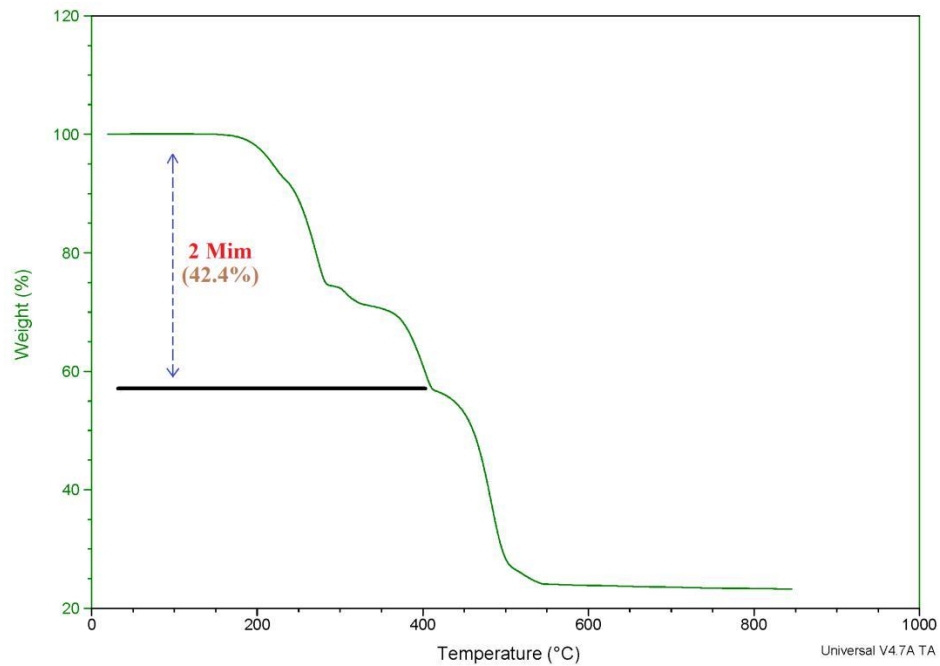


Fig. S2: TGA profile of as synthesized **1** under N<sub>2</sub> flow (40 mL/min).

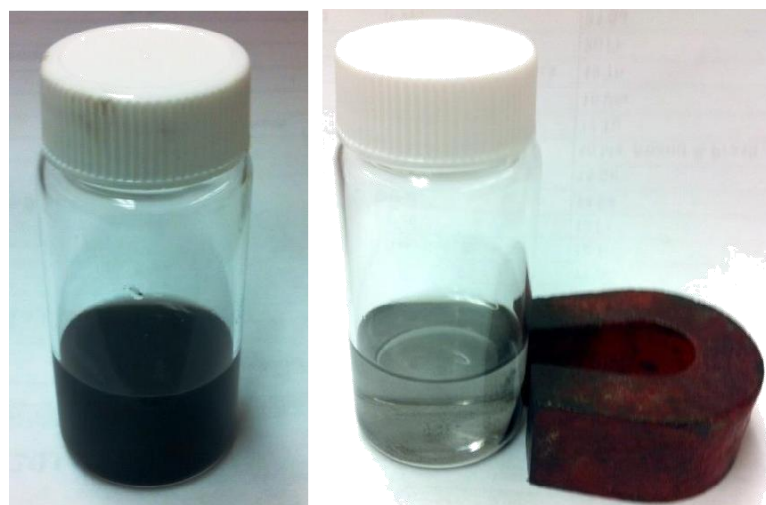


Fig. S3: Physical separation of a suspension of **2** in ethanol with a horse shoe magnet.

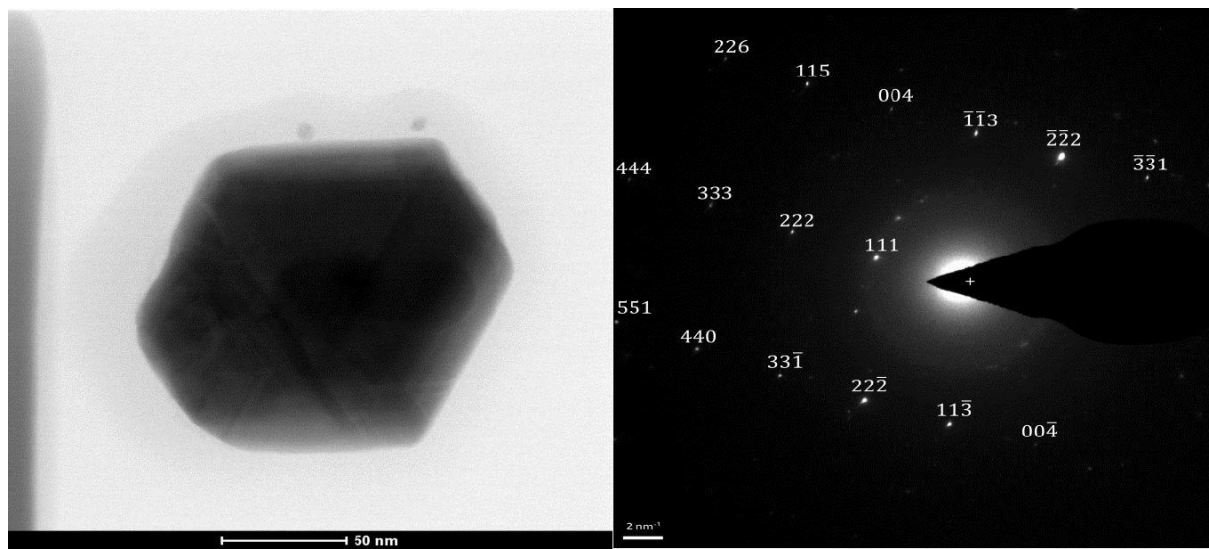


Fig. S4: STEM image of a single Co nanoparticle (left) and its electron diffraction pattern indexed to cubic cobalt; viewed along [111] zone axis (right).

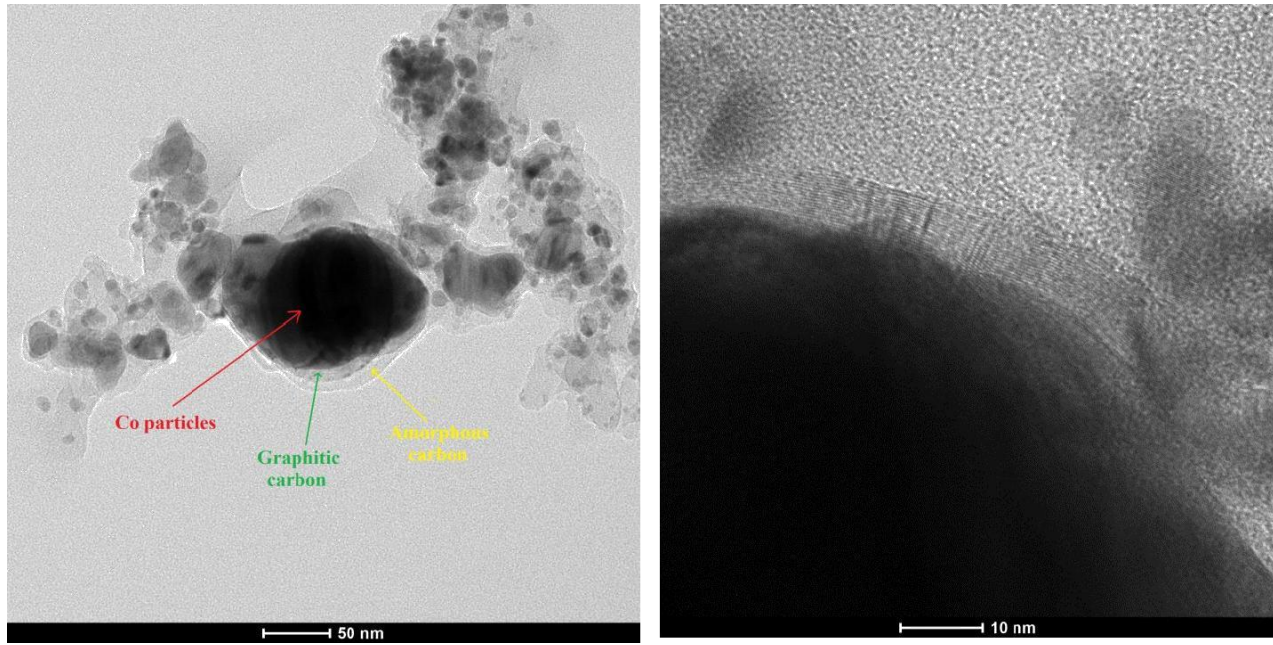


Fig. S5: TEM image of as synthesized **2** showing different region for Co particles embedded by graphitic and amorphous carbon (left) and TEM micrographs for lattice fringes along the boundary region showing the presence of graphitic carbon shell over cobalt particles.

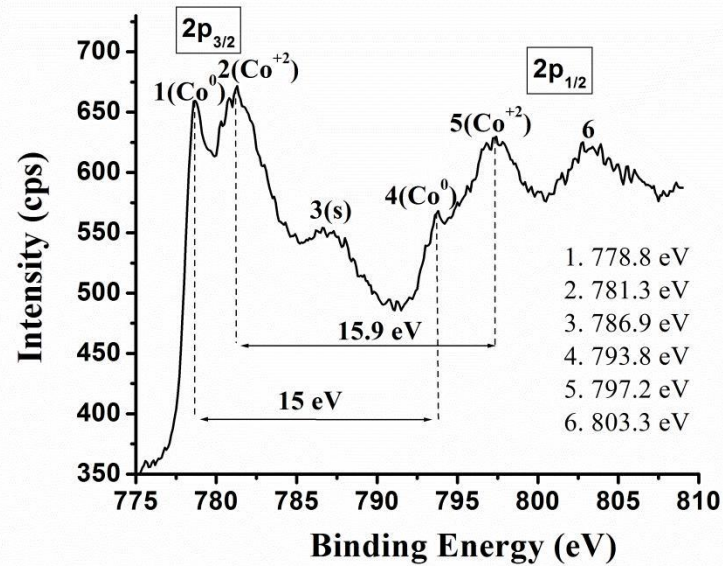


Fig. S6. Cobalt 2p XPS spectrum of **2** without Ar sputtering. Peaks assigned are listed numerically in the inset. Metallic cobalt ( $\text{Co}^0$ ), divalent cobalt ( $\text{Co}^{+2}$ ), and  $\text{Co}^{+2}$  shake-up satellites (s) are labelled.  $\text{Co}_2^{+2}$  peaks are noted to have formed from slow oxidation of reactive metallic cobalt with oxygen.

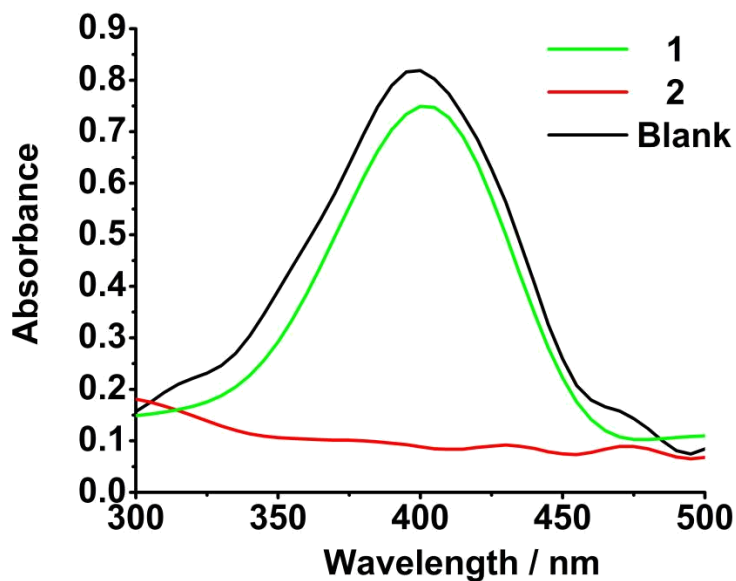


Fig. S7: Reduction of PNP to PAP with **1** (green line), **2** (red line) and in absence of any catalyst (black line).

Table S4: Comparison of rate constants for support and supported catalyst.

Entry	Catalyst	$S_{BET}$ ( $m^2 g^{-1}$ )	$K_{app}$ (min $^{-1}$ )	References
1.	Carbon nanotube (CNT)	176.7	0.001	Gu et. al. Nanoscale, 2014, 6, 6609. [3]
2.	Carbon sphere	13	0.0	Tang et. al. J. Mater. Chem., 2010, 20, 5436. [4]
3	RGO (metal free)	-	0.0	Nie et. al. Carbon, 2012, 50, 586. [5]
2	Pd-NP/CNT	220.5	0.632	Gu et. al. Nanoscale, 2014, 6, 6609. [3]
3	Au/C	770	0.60	Guo et. al. Chem. Commun., 2012, 48, 11094. [6]
4	Au@SiO <sub>2</sub>	nd*	0.234	Lee et. al. Adv. Mater., 2008, 20, 1523. [7]
5	Co@SiO <sub>2</sub>	20.2	0.815	Yan et. al. Inorg. Chem. 2014, 53, 9073. [8]
6	Co@C	128	0.34	This work

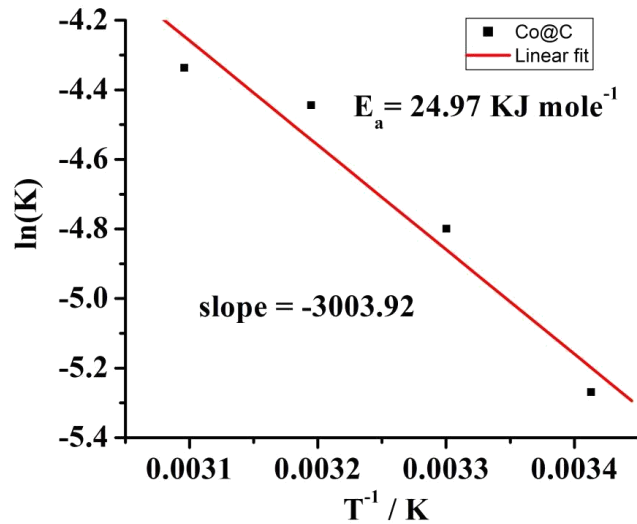


Fig. S8: Reduction of PNP to PAP with **2** (red line) and in absence of any catalyst (black square).

Table S5: Comparison of activation energy among metal supported nanoparticles.

S1 No.	Catalyst (carrier)	$C_{PNP}$ [M]	$C_{BH_4}$ [M]	$E_a$ [KJ mole <sup>-1</sup> ]	References***
1	AgNP	$6.0 \times 10^{-5}$	$2.5 \times 10^{-3}$	41.0	Pradhan et. al [9]
2	AuNP (PMMA beads)	$4.9 \times 10^{-5}$	$7.2 \times 10^{-2}$	38.0	Kuroda et. al [10]
3	AuNP (Ca-alignate stabilized)	$1.0 \times 10^{-4}$	$1.0 \times 10^{-1}$	20.5	Saha et. al [11]
4	Pt-cubes (colloidal)	$1.9 \times 10^{-5}$	$3.2 \times 10^{-2}$	12.0	Mahmoud et. al [12]
5	Pd NP ( $Al_2O_3$ )	$1.0 \times 10^{-4}$	$1.3 \times 10^{-2}$	43.0	Arora et. al [13]
6	Ni NP (hydrogel network)	$1.4 \times 10^{-2}$	$2.9 \times 10^{-1}$	25.7	Sahiner et. al [14]
7	Co NP (hydrogel network)	$1.4 \times 10^{-2}$	$2.9 \times 10^{-1}$	27.8	Sahiner et. al [15]
8	Co@C	$3.7 \times 10^{-5}$	$3.7 \times 10^{-2}$	24.9	This work

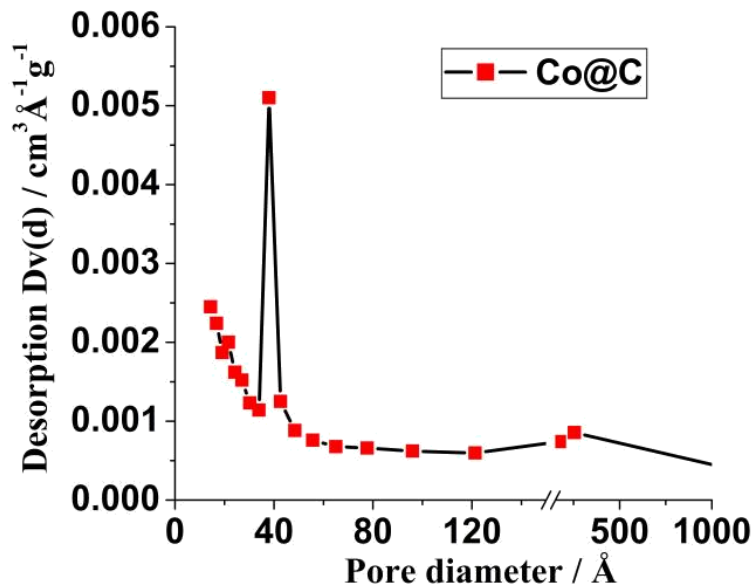


Fig S9: Pore diameter distribution of **Co@C (2)** calculated using BJH method.

## **References:**

- [1]. M. C. Biesinger, B. P. Payne, A. P. Grosvenor, L. W. M. Lau, A. R. Gerson, R. St. C. Smart, *Appl. Surf. Sci.*, **2011**, 257, 2717.
- [2]. N. L. Torad , M. Hu, S. Ishihara, H. Sukegawa, A. A. Belik, M. Imura, K. Ariga, Y. Sakka and Y. Yamauchi, *Small*, **2014**, 10, 2096.
- [3] Xianmo Gu, Wei Qi, Xianzhu Xu, Zhenhua Sun, Liyun Zhang, Wei Liu, Xiaoli Pan, Dangsheng Su, *Nanoscale*, **2014**, 6, 6609.
- [4] Shaochun Tang, Sascha Vongehr, Xiangkang Meng, *J. Mater. Chem.*, **2010**, 20, 5436.
- [5] Renfeng Nie, Junhua Wang, Lina Wang, Yu Qin, Ping Chen, Zhaoyin Hou, *Carbon*, **2012**, 50, 586.
- [6] Jinrui Guo, Kenneth S. Suslick, *Chem. Commun.*, **2012**, 48, 11094.
- [7] Joongoo Lee, Ji Chan Park, Hyunjoon Song, *Adv. Mater.*, **2008**, 20, 1523.
- [8] Nan Yan, Ziang Zhao, Yan Li, Fang Wang, Hao Zhong, Qianwang Chen, *Inorg. Chem.* **2014**, 53, 9073.
- [9] Pradhan, N., Pal, A., Pal, T., *Colloid Surf. B*, **2002**, 196, 247.
- [10] Kuroda, K., Ishida, T., Haruta, M., *J. Mol. Catal. A-Chem.*, **2009**, 298, 7.
- [11] Saha, S., Pal, A., Kundu, S., Basu, S., Pal, T., *Langmuir*, **2010**, 26, 2885.
- [12] Mahmoud, M.A., Snyder, B., El-Sayed, M. A., *J. Phys. Chem. Lett.*, **2010**, 1, 28.
- [13] Arora, S., Kapoor, P., Singla, M.L., *React. Kinet. Mech. Cat.*, **2010**, 99, 157.
- [14] Sahiner, N., Ozay, H., Ozay, O., Aktas, N., *Appl. Catal., A*, **2010**, 385, 201.
- [15] Sahiner, N., Ozay, H., Ozay, O., Aktas, N., *Appl. Catal., B*, **2010**, 101, 137.